Theoretical elastic stiffness of quaternary crystal $Y_3Si_5N_9O$ by first-principles investigation

Jingyang Wang,[1,2,*] Yanchun Zhou,[2,†] Zhijun Lin,[2] and Takahisa Ohno[3]
[1]*International Center for Young Scientists (ICYS), National Institute for Materials Science, Tsukuba, Ibaraki 305-0044, Japan*
[2]*High-Performance Ceramic Division, Shenyang National Laboratory for Materials Science, Institute of Metal Research, Chinese Academy of Sciences, Shenyang 110016, China*
[3]*National Institute for Materials Science, Tsukuba, Ibaraki 305-0047, Japan*
(Received 3 September 2007; revised manuscript received 15 January 2008; published 25 March 2008)

The theoretical elastic stiffness of $Y_3Si_5N_9O$, the only Y-Si-O-N quaternary crystal that contains a framework of corner-sharing SiN_4 and/or $SiON_3$ tetrahedron in three dimensions, was investigated using the first-principles total energy calculations. The full set of second order elastic coefficients, polycrystalline bulk and shear moduli, and anisotropic elastic moduli were reported and further compared with those of Y_2O_3 and β-Si_3N_4. The equation of state and compressibility of $Y_3Si_5N_9O$ were investigated at pressures up to 50 GPa. The crystal structure is stable up to 50 GPa and exhibits anisotropic compressibility under hydrostatic pressure. The relatively softer YN_6 and/or YN_5O polyhedra are more prone to distort or deform than the SiN_4 and/or $SiON_3$ tetrahedra. Therefore, although the crystal structure of $Y_3Si_5N_9O$ contains a Si-N-O framework similar to that in β-Si_3N_4, it displays elastic stiffness between those of Y_2O_3 and β-Si_3N_4.

DOI: 10.1103/PhysRevB.77.104117 PACS number(s): 81.05.Je, 62.20.D−, 71.20.Ps

The oxide of yttrium is one of the typical sintering additives in the densification of silicon nitride. As a result of heat treatment of samples, compounds in the Y-Si-O-N system were frequently identified as precipitate intergranular phases in the grain boundary of bulk Si_3N_4.[1–5] These compounds include two ternary silicates ($Y_2Si_2O_7$ and Y_2SiO_5) and five quaternary phases ($Y_2Si_3N_4O_3$, $Y_4Si_2O_7N_2$, $Y_5Si_3O_{12}N$, $YSiO_2N$, and $Y_3Si_5N_9O$) within the interior of the SiO_2-Y_2O_3-Si_3N_4-YN phase equilibrium diagram. Ching and co-workers first carried out comprehensive theoretical investigations on the Y-Si-O-N system.[1–5] They systematically studied the crystal structure, electronic structure and bonding, and optical properties of all identified eleven compounds in the Y-Si-O-N system and highlighted remarkable correlations between chemical bonding and material properties. These studies provide useful insights into the understanding of structural ceramics at the electronic structure level.

The complex Y-Si-O-N phases can dominate the mechanical and dielectrical properties of polycrystalline Si_3N_4. Recently, the mechanical properties of a model of Y-doped intergranular glassy films (IGFs) in Si_3N_4 were studied by an accurate large-scale first-principles simulation.[6] The results showed that Y-doped IGF enhanced its elastic properties under uniaxial strains compared to the undoped IGF. Very recently, the present authors investigated the theoretical mechanical properties and atomistic shear deformation mechanisms of γ-$Y_2Si_2O_7$ using the first-principles total energy calculations.[7] γ-$Y_2Si_2O_7$ shows an unusual low shear deformation resistance, which endows this ternary compound with quasiductility and good damage tolerance. In addition, γ-$Y_2Si_2O_7$ displays superior mechanical properties compared to α-SiO_2 and may serve as a ductile intergranular phase in polycrystalline Si_3N_4. These works opened a door to strengthen or optimize intergranular phases of Si_3N_4 with improved toughness. Further investigations are urgent in order to customize tailor-made mechanical properties of Si_3N_4 by controlling the chemical composition and crystal structure of intergranular phases.

In contrast to the well-documented crystal structure, electronic structure, and optical property of Y-Si-O-N quaternary crystals, the mechanical properties of these compounds were not referenced in literature for many years. The difficulties lie in two aspects: In actual laboratory experiments, it was extremely difficult to process full dense bulk Y-Si-O-N quaternary crystals; in theoretical calculation, these quaternary compounds crystallize in complex crystal structures with unit cells containing a large number of atoms and yield very low symmetries. Fortunately, mechanical properties of crystals can be calculated and predicted precisely by means of first-principles total energy calculation now. As a first step toward a complete study of the properties of the Y-Si-O-N system, we focused on the $Y_3Si_5N_9O$ quaternary crystal in the present paper. Liddell and Thompson first determined the crystal structure of $Y_3Si_5N_9O$ in 2001,[8] and later in 2005, Ching *et al.* theoretically investigated the electronic structure and bonding characteristics.[5] The reasons why we are interested in this compound are as follows: It has high N content $[N/(N+O)=0.9]$ distinguishing itself from the other four quaternary crystals and, moreover, its local structure is closer to those at the interface of bulk Si_3N_4 and the IGF. Besides, $Y_3Si_5N_9O$ is the only Y-Si-O-N quaternary crystal that contains a framework of corner-sharing SiN_4 and/or $SiON_3$ tetrahedra extending in three dimensions.[5,8] Therefore, a complete investigation of $Y_3Si_5N_9O$ is essential for understanding the properties of intergranular phases in Si_3N_4.

To investigate the theoretical elastic stiffness of $Y_3Si_5N_9O$, we accomplished calculations of a full set of second order elastic coefficients, polycrystalline bulk and shear moduli, and anisotropic Young's moduli. The equation of state and compressibility of $Y_3Si_5N_9O$ were investigated at hydrostatic pressures up to 50 GPa. We compared the mechanical parameters of $Y_3Si_5N_9O$ with those of Si_3N_4 and Y_2O_3 that contain cation-anion bonding of Si-N and Y-O bonds, respectively. In addition, pressure dependences of bond length changes were studied for a better understanding of mechanical property features. The aim of this work is to illustrate the relationships between crystal structure, chemi-

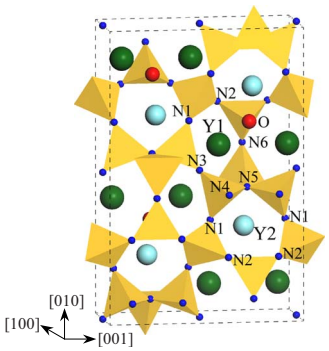

FIG. 1. (Color online) Crystal structure of $Y_3Si_5N_9O$. The cation-anion coordinations are as follows: Y1 is coordinated by N1, N2, N3, N4, N6, and O1; Y2 by two N1, two N2, N5, and O1; Si1 by two N1 and two N2; Si2 by two N2, N6, and O1; Si3 by N1, N3, N4, and N5; and Si4 by two N4, N5, and N6. The Si atoms are located at the center of SiN_4 and $SiON_3$ tetrahedra.

cal bonding, and mechanical properties for $Y_3Si_5N_9O$.

The crystal structure of $Y_3Si_5N_9O$ is shown in Fig. 1. The compound crystallizes in an orthorhombic symmetry (space group 57, *Pbcm*). The unit cell contains four formulas, and there are two Y sites, four Si sites, six N sites, and one O site. The Y ions have the bonding configuration of Y-ON_5, forming the YON_5 polyhedron [Y(1) is coordinated by N(1), N(2), N(3), N(4), N(6), and O(1); Y(2) is coordinated by two N(1), two N(2), N(5), and O(1)]; Si ions show the bonding configurations of either Si-N_4 or Si-ON_3, forming the SiN_4 and $SiON_3$ tetrahedra, respectively. Adjacent SiN_4 or $SiON_3$ tetrahedra share O or N atoms at the corner, forming a framework extending in three dimensions. In addition, the YON_5 polyhedron can be regarded as located at the interstitial sites of the SiN_4 (or $SiON_3$) framework.

The VASP code was used in the present calculations,[9] wherein the projector augmented wave potentials were employed. The special point sampling integration over the Brillouin zone was employed by using the Monkhorst-Pack method with a $5\times2\times2$ special k-point mesh.[10] The $Y_3Si_5N_9O$ unit cell was fully optimized in order to obtain the equilibrium crystal structure. Lattice parameters and internal atomic coordinates were independently modified to minimize the total energy and interatomic forces. The convergence criterion for the total energy was 5.0×10^{-6} eV with a 500 eV cutoff and a maximum stress within 0.01 GPa.

The second order elastic coefficients were determined by means of the linear fitting of the stress-strain relationship. We applied a set of given homogeneous deformations with finite values and calculated the generated stresses after optimizing the internal degrees of freedom. The strains were introduced by transforming the unstrained primitive vectors $\boldsymbol{a}_i$ ($i=1$, 2, and 3) of the unit cell to the newly strained vectors $\boldsymbol{a}_i'$ according to

$$\begin{pmatrix} a_1' \\ a_2' \\ a_3' \end{pmatrix} = \begin{pmatrix} a_1 \\ a_2 \\ a_3 \end{pmatrix} \cdot (I+\varepsilon), \tag{1}$$

where $\boldsymbol{\varepsilon}$ is the applied strain tensor,

TABLE I. Atomic positions for $Y_3Si_5N_9O$: $a=4.934$ Å, $b=16.033$ Å, and $c=10.588$ Å; space group: *Pbcm*.

Atom	Wyckoff	x	y	z
Y(1)	8(e)	0.1630	0.6000	0.5722
Y(2)	4(d)	0.2023	0.7036	0.2500
Si(1)	4(c)	0.6816	0.7500	0.5000
Si(2)	4(d)	0.7497	0.6704	0.7500
Si(3)	8(e)	0.3953	0.4233	0.6033
Si(4)	4(d)	0.8882	0.4726	0.7500
O(1)	4(d)	0.4140	0.6673	0.7500
N(1)	8(e)	0.4737	0.6709	0.4440
N(2)	8(e)	0.8906	0.7178	0.6209
N(3)	4(b)	0.5000	0.5000	0.5000
N(4)	8(e)	0.9493	0.5681	0.3804
N(5)	4(d)	0.4435	0.5633	0.2500
N(6)	4(d)	0.9022	0.5758	0.7500

$$\boldsymbol{\varepsilon} = \begin{pmatrix} \varepsilon_{11} & \frac{\varepsilon_{12}}{2} & \frac{\varepsilon_{13}}{2} \\ \frac{\varepsilon_{12}}{2} & \varepsilon_{22} & \frac{\varepsilon_{23}}{2} \\ \frac{\varepsilon_{13}}{2} & \frac{\varepsilon_{23}}{2} & \varepsilon_{33} \end{pmatrix}. \tag{2}$$

$Y_3Si_5N_9O$ crystallizes in the space group of *Pbcm*, and it has nine independent second order elastic coefficients. The present calculation used the following strain patterns to deduce all these independent elastic coefficients:

$$\text{(i) choosing } \varepsilon_{11}=\varepsilon_{23}=\varepsilon\neq0,$$

$$\text{(ii) choosing } \varepsilon_{22}=\varepsilon_{13}=\varepsilon\neq0,$$

$$\text{(iii) choosing } \varepsilon_{33}=\varepsilon_{12}=\varepsilon\neq0, \tag{3}$$

For each strain pattern, six amplitudes ε, three positive and three negative values, were applied to the unit cell by $|\boldsymbol{\varepsilon}|$, taking 0.1%, 0.3%, and 0.5%.

The present calculation scheme was successfully used to predict the crystal structure, elastic stiffness, and interatomic force constants of ternary carbides[11–13] and complex $LaPO_4$ monazite,[14] $Y_2Si_2O_7$,[7] and $La_2Zr_2O_7$ pyrochlore.[15] Polycrystalline bulk modulus B and anisotropic Young's moduli E were computed from the compliance tensor S and the inverse of stiffness tensor C, $S=C^{-1}$. The polycrystalline shear modulus G was determined according to the Voigt approximation.[16]

Theoretical lattice constants of $Y_3Si_5N_9O$ are listed in Table I. The computed lattice constants ($a=4.934$ Å, $b=16.033$ Å, and $c=10.588$ Å) are in good agreement with experimental data [$a=4.9697$ Å, $b=16.1192$ Å, and $c=10.6277$ Å (Ref. 8)]: $\Delta a/a<0.8\%$, $\Delta b/b<0.6\%$, and $\Delta c/c<0.4\%$. The internal atomic coordinates for $Y_3Si_5N_9O$ are also included in Table I, and the values are consistent with experimental data (see Table II of Ref. 8 for details).

TABLE II. Theoretical second order elastic coefficients of $Y_3Si_5N_9O$, β-Si_3N_4, and Y_2O_3, together with experimental data of β-Si_3N_4 and theoretical values of Y_2O_3 for comparison. All values in GPa.

Compound	c_{11}	c_{12}	c_{44}	c_{13}	c_{33}	c_{66}	c_{22}	c_{23}	c_{55}
$Y_3Si_5N_9O$	319	90	111	116	344	107	363	119	118
β-Si_3N_4	446	181	112	125	580	132			
β-Si_3N_4[a]	433	195	108	127	574	119			
Y_2O_3	227	125	75						
Y_2O_3[b]	242	128	85						

[a]Reference 17.
[b]Reference 18.

These results confirm the reliability of present first-principles calculations to reproduce the equilibrium crystal structure of $Y_3Si_5N_9O$.

The elastic stiffness determines the response of a crystal to an applied strain (or stress) and provides information about bonding characteristics near equilibrium state. The investigation on the elastic stiffness is essentially the first step to understand the mechanical properties of a solid. Table II summarizes the full set of theoretical second order elastic coefficients of $Y_3Si_5N_9O$, Y_2O_3, and β-Si_3N_4, together with the experimental data of β-Si_3N_4 (Ref. 17) and theoretical values of Y_2O_3 (Ref. 18) included to illustrate the accuracy of theoretical results. Our theoretical elastic coefficients of β-Si_3N_4 and Y_2O_3 agree well with reported data. The results support the reliability of present calculations. It should be noted that elastic coefficients of $Y_3Si_5N_9O$ are located between the corresponding values of Y_2O_3 and β-Si_3N_4. For example, the elastic moduli representing the stiffness against uniaxial strains c_{11}, c_{22}, and c_{33} of $Y_3Si_5N_9O$ are, respectively, 319, 363, and 344 GPa, which are 92, 136, and 107 GPa higher than c_{11} of Y_2O_3 ($c_{11}=c_{22}=c_{33}=227$ GPa), respectively, but are 127, 83, and 236 GPa lower than the corresponding values of β-Si_3N_4 ($c_{11}=c_{22}=446$ GPa and $c_{33}=580$ GPa), respectively. The c_{44}, c_{55}, and c_{66} of $Y_3Si_5N_9O$, which correspond to the resistance against shear deformations, are 111, 118, and 107 GPa, respectively, which are also 36, 43, and 32 GPa higher than the c_{44} of Y_2O_3 ($c_{44}=c_{55}=c_{66}=75$ GPa), respectively, but close to c_{44} and c_{55} ($c_{44}=c_{55}=112$ GPa), and 25 GPa lower than c_{66} (=132 GPa) of β-Si_3N_4, respectively.

Bulk modulus measures the resistance of a material to a volume change and provides an estimate of its elastic response to a hydrostatic pressure; shear modulus describes the resistance of a material to a shape change, and Young's modulus reflects the resistance against the uniaxial tensions or compressions. These parameters are important quantities to define the mechanical properties of a material. Table III presents the computed mechanical parameters (including polycrystalline bulk modulus B and shear modulus G, and anisotropic Young's moduli E) of $Y_3Si_5N_9O$, Y_2O_3, and β-Si_3N_4. $Y_3Si_5N_9O$ shows pronounced enhancements of mechanical properties compared to Y_2O_3. For instance, $Y_3Si_5N_9O$ yields bulk modulus B and shear modulus G of 186 and 114 GPa, respectively, which are 26 and 49 GPa higher than those of Y_2O_3 ($B=160$ GPa and $G=65$ GPa). However, B and G of $Y_3Si_5N_9O$ are 72 and 27 GPa lower than those of β-Si_3N_4 ($B=258$ GPa and $G=141$ GPa). In addition, the Young's moduli of $Y_3Si_5N_9O$ vary between those of Y_2O_3 and β-Si_3N_4.

To study the structural stability and compressibility of $Y_3Si_5N_9O$, the equation of state was studied by examining the volume contractions at pressures up to 50 GPa. Hydrostatic pressure was applied to the unit cell. Figure 2 displays the relative unit cell volume V/V_0 as a function of external pressure. The bulk modulus B_0 and its pressure derivative B_0' were determined to be 191 GPa and 3.47, respectively, by fitting the data with the Birch-Murnaghan equation. The fitted bulk modulus agrees well with the value calculated from second order elastic coefficients, as listed in Table III. Figure 3 presents the contractions of lattice constants a, b, and c at various pressures. It is obvious that unit cell volume and lattice constants decrease smoothly with pressure in Figs. 2 and 3, and it indicates that the crystal structure of $Y_3Si_5N_9O$ is stable up to a pressure of 50 GPa. No abrupt changes of crystal structure were observed throughout the investigated pressures.

Figure 3 shows that lattice constant a decreases faster than b and c, which implies that $Y_3Si_5N_9O$ is softer along the a direction. In addition, the shrinkages of $Y_3Si_5N_9O$ under pressure are almost identical in b and c directions. The origin of anisotropic compressibility can be attributed to the different bonding characteristics along various directions, which are illustrated in Fig. 4. As shown in Fig. 4(a), the Y atomic plane and Si-N-O framework alternatively stack along the [100] direction; on the other hand, the Y atoms are located in the interstitial sites of the Si-N-O framework in Fig. 4(b),

TABLE III. Theoretical polycrystalline bulk modulus B and shear modulus G, and anisotropic Young's moduli of $Y_3Si_5N_9O$, Y_2O_3, and β-Si_3N_4

Compound	B (GPa)	G (GPa)	E (GPa)
$Y_3Si_5N_9O$	186	114	$E_x=272$
			$E_y=313$
			$E_z=280$
β-Si_3N_4	258	141	$E_x=362$
			$E_z=530$
Y_2O_3	160	65	$E_x=139$

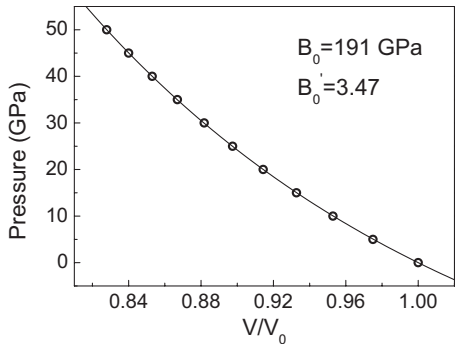

FIG. 2. Pressure dependence of volume contraction V/V_0. Bulk modulus B_0 and its pressure derivative B_0' were determined to be 191 GPa and 3.47, respectively, by fitting the data with the Birch-Murnaghan equation.

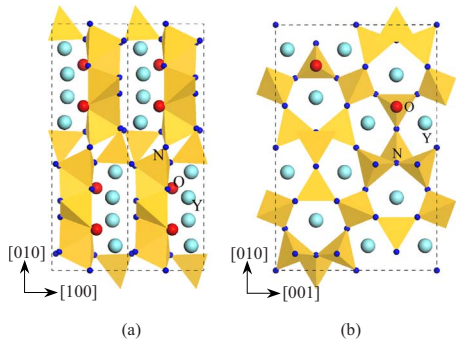

FIG. 4. (Color online) Schematic illustrations of different bonding characteristics along various projections of the (a) [001] direction and (b) [100] direction.

which illustrates the stacking configuration of the *bc* plane. Figure 4(b) shows that the corner-sharing Si-N-O framework is almost isotropic along the [010] and [001] directions. It is expected that the Y-N and/or Y-O bond/s is/are relatively softer than the Si-N and/or Si-O bond/s. Therefore, $Y_3Si_5N_9O$ is relatively softer along the *a* direction and is almost of the same compressibility along *b* and *c* directions.

In order to study the physical origin of the characteristics of mechanical properties, the information of the response of bonds to applied strain is essential. We aimed to reveal which bonds are prone to distort for $Y_3Si_5N_9O$ under mechanical perturbations. The present work investigates the resistances of bonds to applied hydrostatic pressures. Table IV illustrates the bond length contractions of cation-anion bonds (normalized by equilibrium values at zero pressure) at a pressure of 50 GPa. The cation-anion bond pairs are classified according to bonding configurations in $Y_3Si_5N_9O$ (in the same way as in Refs. 5 and 8). $Y_3Si_5N_9O$ contains two types of cation-anion bonds in general: the Si-O or Si-N bond/s in the SiN_4 or $SiON_3$ tetrahedra and the Y-O or Y-N bond/s in the YON_5 polyhedra. The values of contractions for Y(1)-N/O and Y(2)-N/O are between 0.908 and 0.953 and 0.920 and 0.992, respectively, and those of Si(1)-N, Si(2)-N/O, Si(3)-N, and Si(4)-N are located between 0.948 and 0.953, 0.958 and 0.959, 0.949 and 0.965, and 0.952 and 0.965,

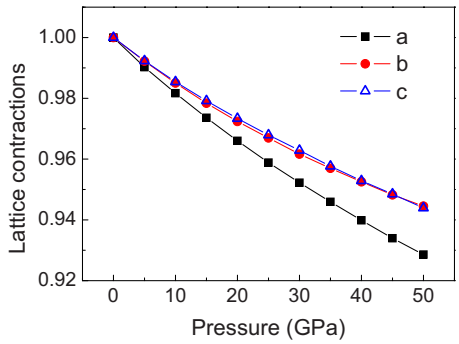

FIG. 3. (Color online) Normalized lattice constant contractions as functions of pressure.

respectively. It is clear that the YN_6 and/or YN_5O polyhedra change more significantly than the SiN_4 and/or $SiON_3$ tetrahedra. Xu *et al.* have discussed the strengths of cation-anion bonds by analyzing the equilibrium bond orders in $Y_3Si_5N_9O$.[5] In brief, the bond orders of Y-O and Y-N bonds were smaller than those of the Si-N and Si-O bonds, and the Y-O and/or Y-N bond/s was/were suggested to be weaker than the Si-N and/or Si-O bond/s in $Y_3Si_5N_9O$. Therefore, relatively softer YN_6 and YN_5O polyhedra are prone to distort under hydrostatic pressure than the SiN_4 and $SiON_3$ tetrahedra framework. Deformation is predominantly accommodated by the YN_6 and/or YN_5O polyhedra when $Y_3Si_5N_9O$ is exposed to pressure.

In conclusion, we studied the theoretical elastic stiffness (including second order elastic coefficients, polycrystalline bulk and shear moduli, anisotropic elastic moduli, equation of state, and compressibility) of $Y_3Si_5N_9O$ using the first-principles total energy calculations. $Y_3Si_5N_9O$ displays mechanical parameters located between the corresponding values of Y_2O_3 and β-Si_3N_4. The relatively soft YN_6 and/or YN_5O polyhedra are prone to distort or deform compared to

TABLE IV. Calculated bond-length contractions of cation-anion pairs at 50 GPa hydrostatic pressure.

Cation	Bond length contractions at 50 GPa hydrostatic pressure			
Y(1)	Y(1)-N(6) 0.948	Y(1)-N(1) 0.953	Y(1)-N(4) 0.944	Y(1)-N(2) 0.945
	Y(1)-N(3) 0.934	Y(1)-O(1) 0.908		
Y(2)	Y(2)-O(1) 0.957	Y(2)-N(2) 0.925	Y(2)-N(1) 0.920	Y(2)-N(5) 0.992
Si(1)	Si(1)-N(2) 0.953	Si(1)-N(1) 0.948		
Si(2)	Si(2)-O(1) 0.958	Si(2)-N(6) 0.958	Si(2)-N(2) 0.959	
Si(3)	Si(3)-N(4) 0.965	Si(3)-N(1) 0.959	Si(3)-N(3) 0.965	Si(3)-N(5) 0.949
Si(4)	Si(4)-N(6) 0.952	Si(4)-N(4) 0.965	Si(4)-N(5) 0.965	

the SiN_4 and/or $SiON_3$ tetrahedra. Therefore, although the crystal structure of $Y_3Si_5N_9O$ contains the Si-N-O framework similar to that in β-Si_3N_4, the material is obviously softer than β-Si_3N_4. Furthermore, the compound exhibits anisotropic compressibility under hydrostatic pressures: The lattice in the *a* direction is more compressible than *b* and *c* directions.

This work was partly supported by the Special Coordination Funds for Promoting Science and Technology from MEXT (J.W., ICYS). Financial support from the National Outstanding Young Scientist Foundation under Grant No. 59925208 (Y.Z.) and the Natural Science Foundation of China under Grants No. 50672102, No. 90403027, and No. 50302011 are acknowledged.

*Corresponding author: jywang@imr.ac.cn
†Corresponding author: yczhou@imr.ac.cn

[1] W. Y. Ching, J. Am. Ceram. Soc. **87**, 1996 (2004).
[2] W. Y. Ching, L. Z. Ouyang, H. Z. Yao, and Y. N. Xu, Phys. Rev. B **70**, 085105 (2004).
[3] W. Y. Ching, L. Z. Ouyang, and Y. N. Xu, Phys. Rev. B **67**, 245108 (2003).
[4] Y. N. Xu and W. Y. Ching, Phys. Rev. B **51**, 17379 (1995).
[5] Y. N. Xu, P. Rulis, and W. Y. Ching, Phys. Rev. B **72**, 113101 (2005).
[6] J. Chen, L. Ouyang, P. Rulis, A. Misra, and W. Y. Ching, Phys. Rev. Lett. **95**, 256103 (2005).
[7] J. Y. Wang, Y. C. Zhou, and Z. J. Lin, Acta Mater. **55**, 6019 (2007).
[8] K. Liddell and D. P. Thompson, J. Mater. Chem. **11**, 507 (2001).
[9] G. Kresse and D. Joubert, Phys. Rev. B **59**, 1758 (1999).
[10] H. J. Monkhorst and J. D. Pack, Phys. Rev. B **13**, 5188 (1976).
[11] J. Y. Wang, Y. C. Zhou, T. Liao, and Z. J. Lin, Appl. Phys. Lett. **89**, 021917 (2006).
[12] T. Liao, J. Wang, and Y. Zhou, Phys. Rev. B **74**, 174112 (2006).
[13] J. Y. Wang, Y. C. Zhou, Z. J. Lin, T. Liao, and L. F. He, Phys. Rev. B **73**, 134107 (2006).
[14] J. Y. Wang, Y. C. Zhou, and Z. J. Lin, Appl. Phys. Lett. **87**, 051902 (2005).
[15] B. Liu, J. Y. Wang, Y. C. Zhou, T. Liao, and F. Z. Li, Acta Mater. **55**, 2949 (2007).
[16] B. Holm, R. Ahuja, Y. Yourdshahyan, B. Johansson, and B. I. Lundqvist, Phys. Rev. B **59**, 12777 (1999).
[17] R. Vogelgesang, M. Grimsditch, and J. S. Wallace, Appl. Phys. Lett. **76**, 982 (2000).
[18] H. Z. Yao, L. Z. Ouyang, and W. Y. Ching, J. Am. Ceram. Soc. **90**, 3194 (2007).